Compact Azimuthal Omnidirectional Dual-Polarized Antenna Using Highly Isolated Colocated Slots

Yue Li, *Student Member, IEEE*, Zhijun Zhang, *Senior Member, IEEE*, Jianfeng Zheng, and Zhenghe Feng, *Fellow, IEEE*

***Abstract*—An omnidirectional dual-polarized antenna with high port isolation is presented for 2.4-GHz wireless local area network (WLAN) applications. The omnidirectional patterns of both vertical and horizontal polarizations in the azimuthal plane are achieved by positioning two orthogonal slots cut onto the walls of a slender columnar cuboid. The overall volume of the proposed antenna is only $83\times11\times11$ mm^3 $(0.664\lambda_0\times0.088\lambda_0\times0.088\lambda_0)$, with low mutual coupling between two radiating slots. A prototype of the proposed antenna is fabricated and tested. The measured results show that the 10-dB reflection coefficient bandwidths of dual polarizations cover the desired band of 2.4–2.48 GHz and the port isolation is lower than -33.5 dB. Stable gains are greater than 3.17 and 1.19 dBi for vertical and horizontal polarizations, respectively. The diversity performance is also evaluated, including the correlation coefficient, mean effective gain (MEG) ratio, and diversity gain.**

***Index Terms*—Antenna diversity, antenna radiation patterns, mutual coupling, slot antennas.**

I. Introduction

In MODERN wireless communication systems, dual-polarized antennas are widely adopted to increase spectrum efficiency and mitigate polarization mismatch between the transmitter and the receiver. In particular, for the multiple-input–multiple-output (MIMO) systems, dual-polarized antennas are usually employed to substitute two specially separated single-polarized antennas, saving the space between them. Such polarized MIMO antennas have been proved to show good performance in increasing the channel capacity and the diversity gain in real MIMO systems [1]–[5]. However, the mutual coupling between different polarizations must be reduced to assure the benefit of MIMO applications.

In recent publications, a series of dual-polarized antennas are designed with different radiating structures, such as the patches [6]–[8] and the slots [9], [10]. Good port isolation is achieved by properly arranging the feeding structures of dual polarizations. The radiation patterns of these designs are unidirectional [6]–[8] or bidirectional [9], [10]. However, to cover a large service area, the antennas with omnidirectional pattern in the azimuthal plane are required in base stations or portable access points.

Different methods are utilized to design omnidirectional antennas with vertical or horizontal polarization. To achieve vertical polarization, a coaxial collinear antenna is investigated in [11], and similar designs using the microstrip [12] and the dipoles [13], [14] are also reported. Another low-profile slot loop antenna with a back cavity is presented in [15]. For the horizontally polarized omnidirectional pattern, the magnetic dipole is a classical solution, achieved by a small loop with a uniform current distribution [16]. However, the impedance of the small loop is difficult to match due to its small dimensions. Other sophisticated structures including the Alford loop structure [17], [18] and the left-handed loading loop [19] are also employed with good impedance matching. Combining the vertically and the horizontally polarized antenna elements is a direct solution to achieve dual omnidirectional polarizations. In [20], a collinear antenna is positioned upward for the vertical polarization, and a slot antenna downward to achieve the horizontal polarization. However, a tilt beam appears in the elevation plane due to the asymmetrical structure. The overall dimension of this antenna is also quite large, which is not suitable for the volume-limited portable devices.

This paper solves two major problems of the MIMO antenna design in a volume-limited system. One is to achieve omnidirectional radiation patterns for both vertical and horizontal polarizations in a small volume, and the other is to reduce the mutual coupling between dual polarizations in such a small volume. Based on these requirements, two colocated slots cutting onto the walls of a slender columnar cuboid are presented to achieve the vertically and the horizontally polarized omnidirectional radiation patterns. Low mutual coupling between dual polarizations is achieved in a small volume of $83\times11\times11$ mm^3 $(0.664\lambda_0\times0.088\lambda_0\times0.088\lambda_0)$. A prototype of the proposed antenna is tested to validate the design strategy. The measured results including S-parameters, radiation patterns, and gain are also reported and discussed.

II. Antenna Design

Fig. 1 shows the geometry and the dimensions of the proposed antenna. As shown in the 3-D view in Fig. 1(a), a metallic columnar cuboid is supported by an FR4 substrate $(\varepsilon_r = 4.4,\ \tan\delta = 0.01)$ in the center. Four walls of the cuboid are named Sides 1–4, with a thickness $t = 1$ mm. The

Manuscript received December 04, 2011; manuscript revised March 30, 2012; accepted April 22, 2012. Date of publication July 03, 2012; date of current version August 30, 2012. This work was supported by the National Basic Research Program of China under Contract 2009CB320205, in part by the National High Technology Research and Development Program of China (863 Program) under Contract 2011AA010202, the National Science and Technology Major Project of the Ministry of Science and Technology of China under Grant 2010ZX03007-001-01, and Qualcomm, Inc.

The authors are with the State Key Laboratory on Microwave and Digital Communications, Tsinghua National Laboratory for Information Science and Technology, Department of Electronic Engineering, Tsinghua University, Beijing 100084, China (e-mail: zjzh@mail.tsinghua.edu.cn; fzh-dee@mail.tsinghua.edu.cn; hardy_723@163.com; zjf98@mails.tsinghua.edu.cn).

Color versions of one or more of the figures in this paper are available online at http://ieeexplore.ieee.org.

Digital Object Identifier 10.1109/TAP.2012.2207072

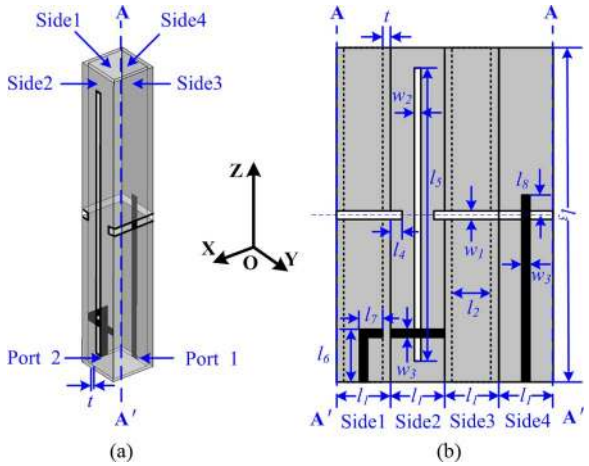

Fig. 1. Geometry and dimensions of the proposed antenna. (a) 3-D view. (b) Expanded view.

TABLE I
DETAILED DIMENSIONS (UNIT: MILLIMETERS)

Parameter	l_1	l_2	l_3	l_4	l_5	l_6
Value	11	9	83	2.9	73	16
Parameter	l_7	l_8	w_1	w_2	w_3	t
value	5.45	3.7	2	1.1	1.9	1

expanded view of the proposed antenna cut along the trace AA' is shown in Fig. 1(b). The dark area expresses the back side, and the light area the front side. A vertical slot is positioned in the center of Side 2, with the dimension $l_5 \times w_2$. A 50-Ω open-ended microstrip line on the back of Sides 1 and 2 is used to feed the vertical slot by capacitive coupling, with the length $(l_6+l_7+l_2)$. Another horizontal slot is positioned in the middle of the cuboid, with the dimension $(l_1\times 3+l_4\times 2)\times w_1$. It is also fed by a 50-Ω open-ended microstrip line on the back of Side 4, with the length $l_3 \times 0.5 + l_8$. The values of each parameter are optimized by using the Ansoft High Frequency Structure Simulator (HFSS) software. The detailed values are listed in Table I. When fed through Port 1, the proposed antenna operates at a vertical polarization mode. The horizontal polarization is provided by feeding the proposed antenna through Port 2. These two colocated slots are able to provide omnidirectional patterns in the azimuthal plane with low mutual coupling and acceptable bandwidth. The volume of the proposed antenna is only $l_3 \times l_1 \times l_1 = 83 \times 11 \times 11$ mm^3.

A. Operating Mechanism

The operating mechanisms of the two slots are different. The horizontal slot is cut onto the walls of all four sides to provide vertically polarized omnidirectional pattern. It is clear that the gain variation in the azimuthal plane varies with different l_1, as shown in Fig. 2(a). The values of maximum minus minimum of gain in each pattern are listed in Table II. By decreasing the value of l_1, a gain variation less than 3 dB can be achieved in xy-plane. However, l_1 also determines the operating frequency of the horizontal slot. Using the values in Table I, the length of the horizontal slot is $l_1\times 3+l_4\times 2 = 38.8$ mm, which is nearly a half of the resonant wavelength (38 mm at 2.4 GHz). The magnitude distributions of current and electric field are shown in

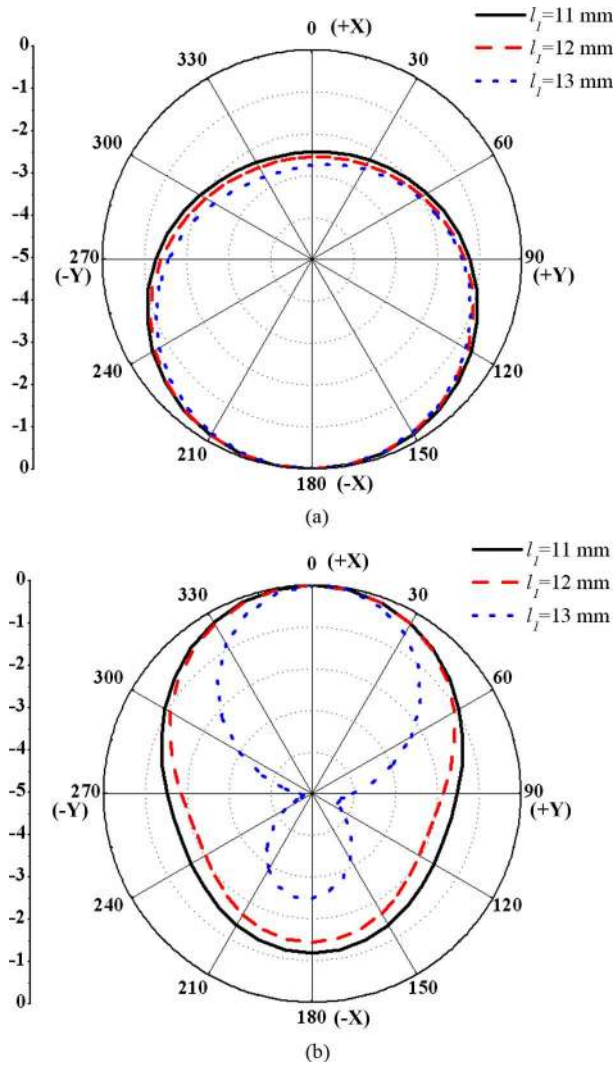

Fig. 2. Simulated normalized radiation pattern in azimuth plane with different l_1 at 2.44 GHz for (a) vertical polarization and (b) horizontal polarization.

TABLE II
GAIN VARIATIONS

Polarization	l_1 = 11 mm	l_1 = 12 mm	l_1 = 13 mm
Vertical	2.43 dB	2.55 dB	2.78 dB
Horizontal	1.67 dB	2.07 dB	4.79 dB

Figs. 3 and 4, and the half-wavelength mode appears in the horizontal slot. The impedance of this mode is matched by tuning the length l_8 of feeding microstrip, shown in Fig. 5. When l_8 equals 3.7 mm, the 10-dB reflection coefficient bandwidth is from 2.29 to 2.59 GHz.

For the horizontal polarization, the vertical slot cut onto the wall of Side 2 also provides a uniform omnidirectional pattern with a small value of l_1, shown in Fig. 2(b). The electric field radiating from the front side can creep along the walls of the slender columnar cuboid to the back side. However, the vertical slot is also difficult to match when l_1 is small. The reason can be the cavity-backed slot antenna model built in Fig. 6. The folded ground can be treated as an open-ended back cavity of the vertical slot. To study the effect of this cavity, the impedance curves are shown in Fig. 7 with different l_1, with other values

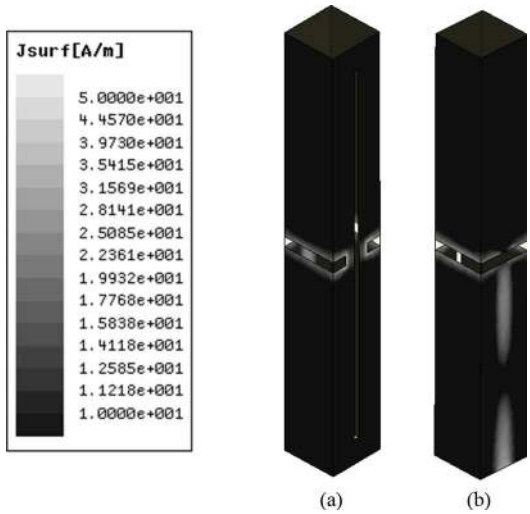

Fig. 3. Current magnitude distribution of the horizontal polarization mode fed through port 1 at 2.44 GHz. (a) Sides 1 and 2. (b) Sides 3 and 4.

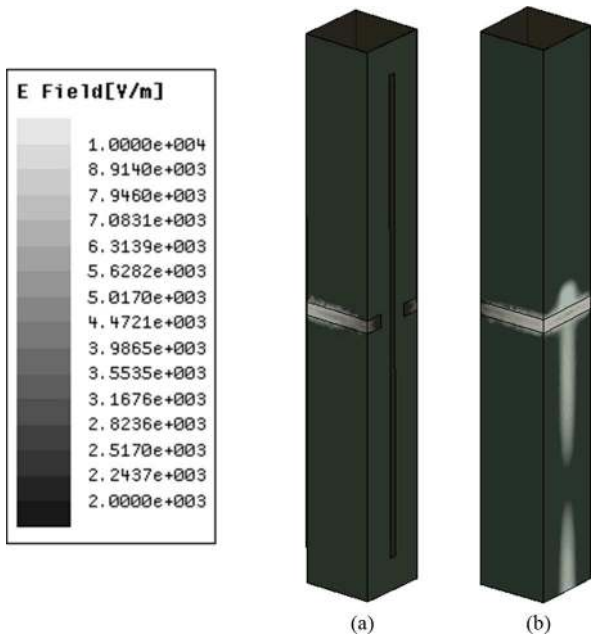

Fig. 4. Electric field magnitude distribution of the horizontal polarization mode fed through port 1 at 2.44 GHz. (a) Sides 1 and 2. (b) Sides 3 and 4.

listed in Table I. With a decrease of l_1, the impedance curve moves out of the VSWR $= 2:1$ circle on the Smith chart. When $l_1 = 5$ mm, the impedance curve moves to the top left corner, with a small value of real part and a large value of image part. To achieve an omnidirectional pattern with $l_1 = 11$ mm, the impedance of the slot is difficult to be matched. There is a conflict between the omnidirectional radiation pattern and the impedance matching.

The open-ended microstrip line is able to match the antenna as a shunt capacitance. Also, the position of feeding (l_6) is helpful in impedance matching. However, it is hard to match the slot in a wide bandwidth. The radiation resistance of the slot is dictated by its length. As shown in Fig. 8, the length of the vertical slot (l_5) is used for wideband impedance matching. All the other parameters use the values of Table I, but with different l_5. With the increase of l_5, the impedance curve moves into the

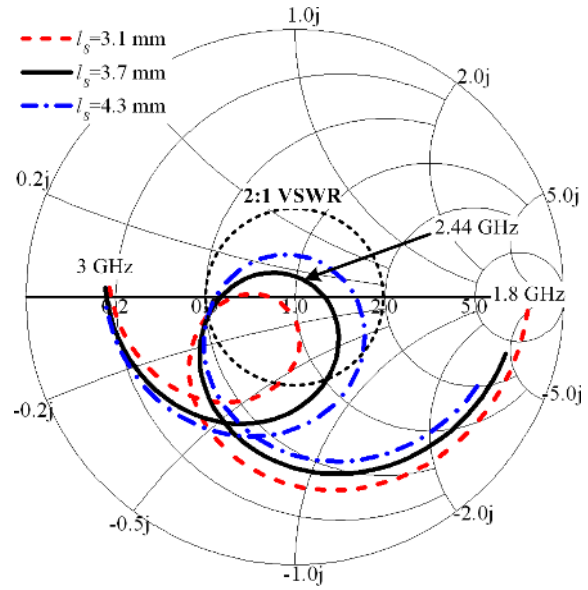

Fig. 5. Impedance curves of the vertical polarization mode on Smith chart with different l_8.

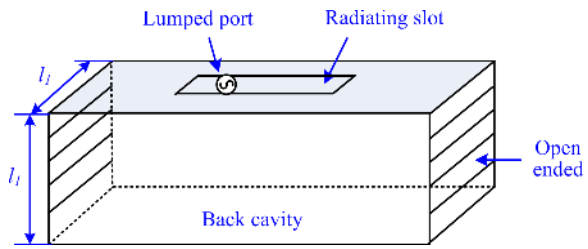

Fig. 6. Antenna model of the slot with back cavity.

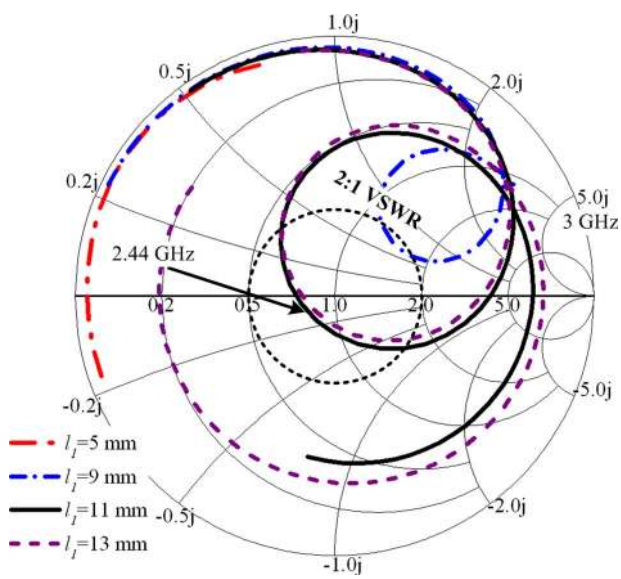

Fig. 7. Impedance curves of the antenna on Smith chart with different l_1 based on the model in Fig. 6.

circle of VSWR $= 2:1$, then moves out of this circle. At an optimized value of 73 mm, the slot has been matched with a 10-dB reflection coefficient bandwidth wider than 2.4–2.48 GHz. Although the length of the vertical slot is nearly one wavelength of 2.4 GHz, the current of the matched slot is still a half-wavelength mode in the desired band, as shown in Fig. 9. For single

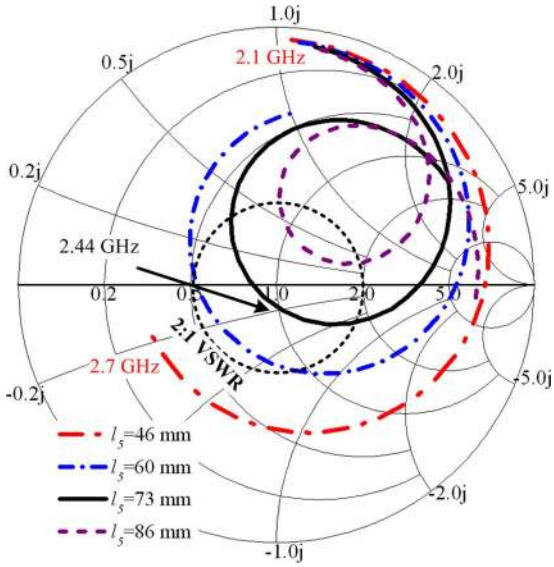

Fig. 8. Impedance curves of the horizontal polarization mode on Smith chart with different l_5.

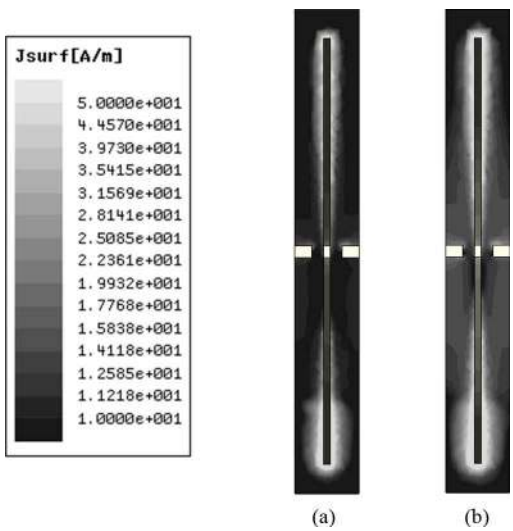

Fig. 9. Current magnitude distribution of the horizontal polarization mode fed through port 2 at (a) 2.4 and (b) 2.48 GHz.

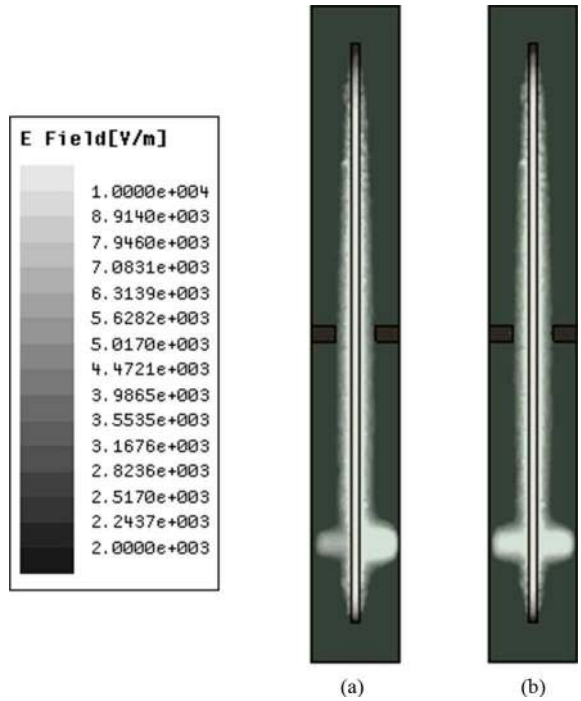

Fig. 10. Electric field magnitude distribution of the horizontal polarization mode fed through port 2 at (a) 2.4 and (b) 2.48 GHz.

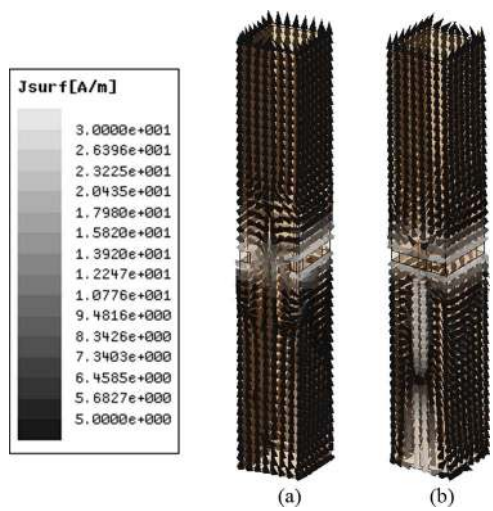

Fig. 11. Vector current distribution of the antenna fed through port 1 at 2.44 GHz on (a) horizontal slot and (b) vertical slot.

73-mm slot without the back cavity, the operation frequency of half wavelength mode is approximately 1.25 GHz. Due to the effect of back cavity and capacitive feeding, the operation frequency of half-wavelength mode is shifted to 2.4 GHz with acceptable bandwidth. Obviously, the electric field magnitude distribution in Fig. 10 also indicates the half-wavelength mode in the vertical slot.

B. Isolation Analysis

The mutual coupling between two radiating element is another important issue in the MIMO antenna design. It is a challenge to achieve high isolation between two ports in such a small volume. To enhance the isolation, the two slots are positioned orthogonally and symmetrically. The current distributions along the colocated slots are investigated to explain the isolation enhancement method. The vector current distributions for both polarizations at 2.44 GHz are shown in Figs. 11 and 12. The current relations of two slots are indicated in Figs. 13 and 14, based on the vector current distributions in Figs. 11 and 12, respectively. When the antenna is fed through Port 1, the current along the horizontal slot is shown in Fig. 13(a). Strong current on the narrow edges is coupled to the middle of the wide edges of the vertical slot. However, the coupled current is with the same amplitude and in phase, as shown in Fig. 13(b). As a result, an extremely weak field is coupled to the vertical slot.

When the antenna is fed through Port 2, the current distributions along two slots are shown in Fig. 14. The vertical slot operates at a half-wavelength mode, and the middle of the wide edge is the current null. The coupled current on the horizontal slot is also in phase along two opposite wide edges. Therefore, the coupled field in the horizontal slot is also very weak. High

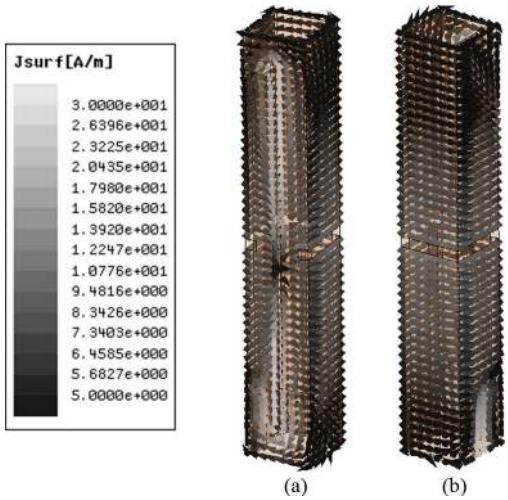

Fig. 12. Vector current distribution of the antenna fed through port 2 at 2.44 GHz on (a) horizontal slot and (b) vertical slot.

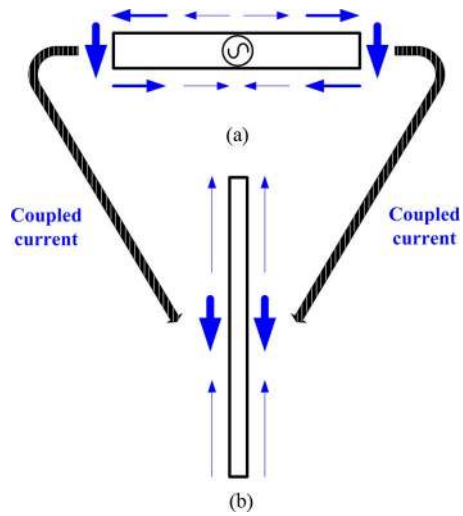

Fig. 13. Current relation of two slots when the antenna fed through port 1 at 2.44 GHz on (a) horizontal slot and (b) vertical slot.

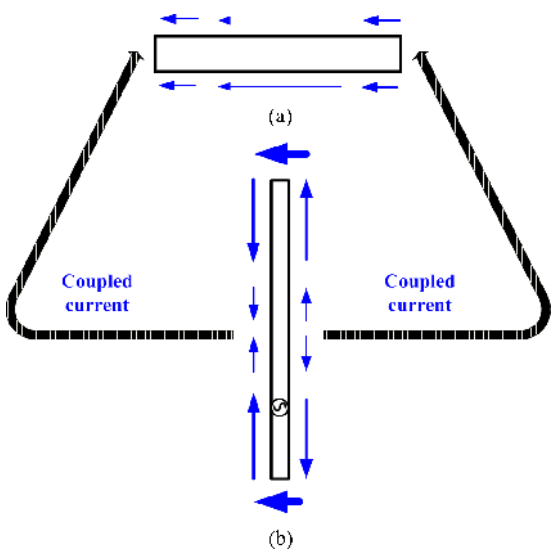

Fig. 14. Current relation of two slots when the antenna fed through port 2 at 2.44 GHz on (a) horizontal slot and (b) vertical slot.

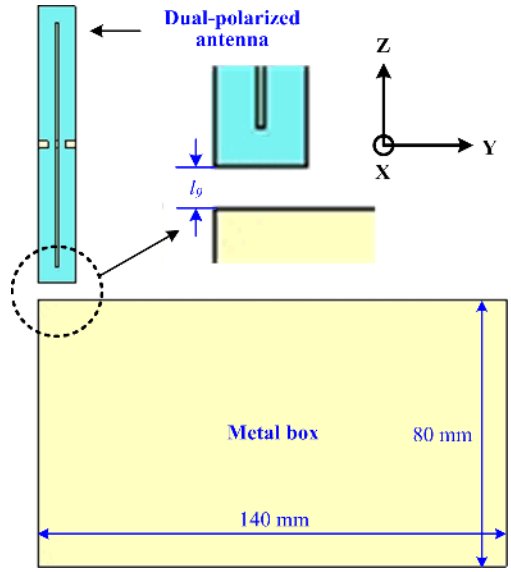

Fig. 15. Antenna application with the ground plane.

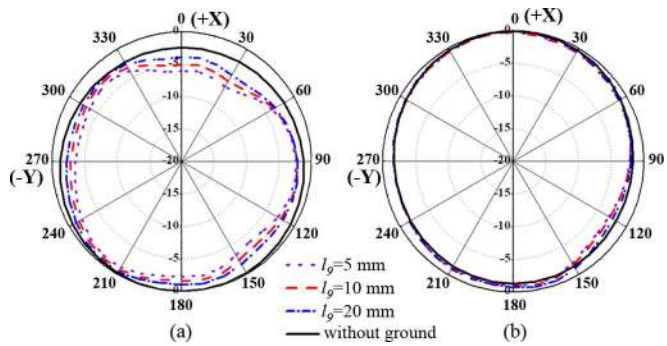

Fig. 16. Simulated normalized radiation pattern for copolarization in azimuth plane with different l_9 at 2.44 GHz when the antenna fed through (a) Port 1 and (b) Port 2.

port isolation can be achieved by this arrangement of colocated slots.

C. Performance Impact of Ground

As mentioned in the Introduction, the proposed antenna is designed for the access points or mobile terminals. For this application, the antenna should be mounted with a large ground plane nearby. The proposed dual-polarized antenna was simulated with a metal box to study the effect the ground plane. As shown in Fig. 15, the antenna is mounted above the metal box with a distance of l_9. The dimensions of the metal box are $140 \times 80 \times 10$ mm^3.

From the simulation results, the ground plane has little effect on the impedance matching (S_{11}, S_{22}) and the ports isolation (S_{21}). However, the radiation patterns of both polarizations vary with different l_9. The simulated normalized radiation patterns in the azimuthal plane at 2.44 GHz are shown in Figs. 16 and 17. Fig. 16 shows the copolarizations, and Fig. 17 shows the cross polarization for both two feeding modes. When the antenna is fed through port 1, the gain variation degrades with the decreasing of l_9. The gain variation is 3.8 dB at $l_9 = 5$ mm, 3.2 dB at $l_9 = 10$ mm and 2.8 dB at $l_9 = 20$ mm. Compared to the value of 2.43 dB (single antenna without the ground plane),

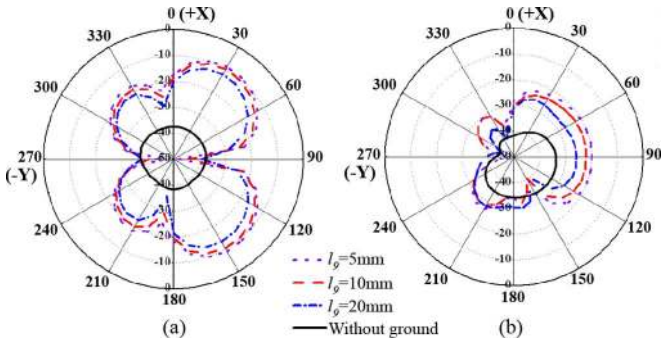

Fig. 17. Simulated normalized radiation pattern for cross polarization in azimuth plane with different l_9 at 2.44 GHz when the antenna fed through (a) Port 1 and (b) Port 2.

Fig. 18. Photograph of the proposed antenna.

the gain variation is still good with a ground plane nearby. When the antenna is fed through port 2, the worst gain variation is 2.8 dB at $l_9 = 5$ mm.

Another effect is the deterioration of the cross polarization. For both of the two modes, the cross polarization increases with the decrease of l_9. When l_9 is 5 mm, the gain levels between copolarization and cross polarization are 10.2 and 19.5 dB for both of the two modes. The results are acceptable for the practical application of access points.

III. Experimental Results

To validate the design strategy, a prototype of the proposed antenna was built and measured, as shown in Fig. 18. The antenna prototype was fed by two 50-Ω coaxial cables. The feeding coaxial cables can be treated as an extension of the ground. To maintain the beam in the azimuthal plane, a series of magnetic beads are used to prevent surface current on the feeding cables.

A. S-Parameters

The measured results of S-parameters are illustrated in Fig. 19, which agreed well with the simulated results. The bandwidths of the reflection coefficient better than -10 dB are 2.31–2.54 GHz for the vertical polarization mode and 2.39–2.49 GHz for the horizontal polarization mode, both covering the 2.4-GHz WLAN band of 2.4–2.48 GHz. In this desired band, the isolation between two feeding port is lower than -33.5 dB. Once again, high port isolation is achieved in a small volume of $83 \times 11 \times 11$ mm^3 $(0.664\lambda_0 \times 0.088\lambda_0 \times 0.088\lambda_0)$.

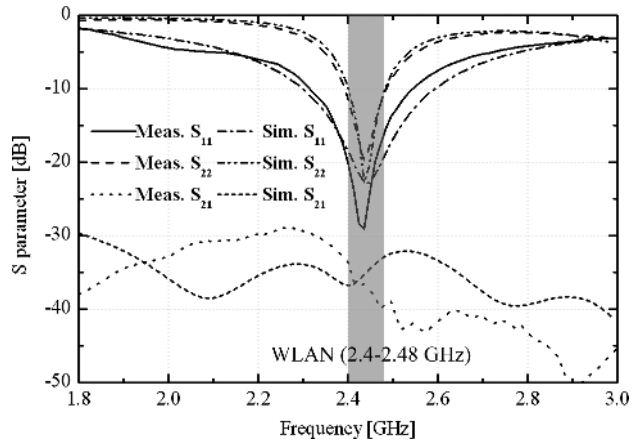

Fig. 19. Measured and simulated S-parameters of the proposed antenna.

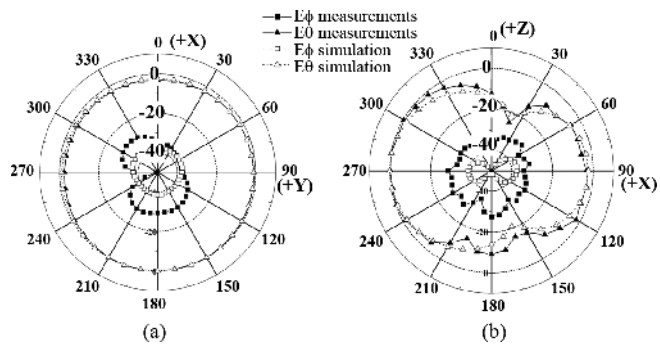

Fig. 20. Simulated and measured radiation patterns of the proposed antenna fed though Port 1 at 2.44 GHz in (a) xy-plane and (b) xz-plane.

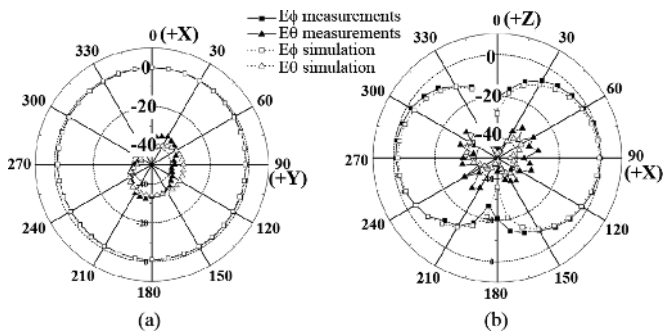

Fig. 21. Simulated and measured radiation patterns of the proposed antenna fed though Port 2 at 2.44 GHz in (a) xy-plane and (b) xz-plane.

B. Radiation Performance

The normalized measured and the simulated radiation patterns of the proposed antenna fed through Ports 1 and Port 2 in the xy- and the xz-planes at 2.44 GHz are shown in Figs. 20 and 21. Clearly, an omnidirectional pattern is achieved in the xy-plane for vertical and horizontal polarizations. The measured values of maximum minus minimum of gain in the xy-plane are 2.9 dB for vertical polarization and 2.1 dB for

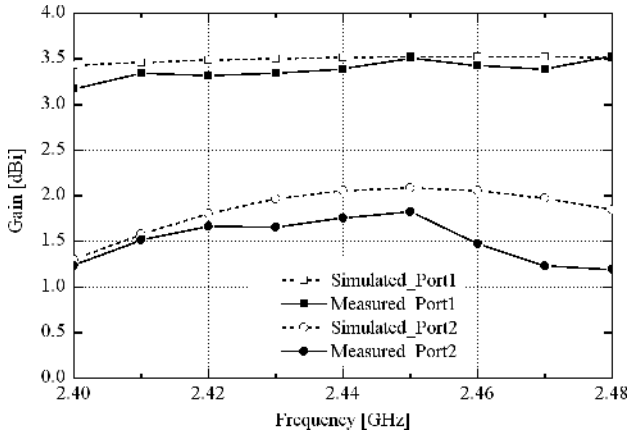

Fig. 22. Simulated and measured gains of the proposed antenna.

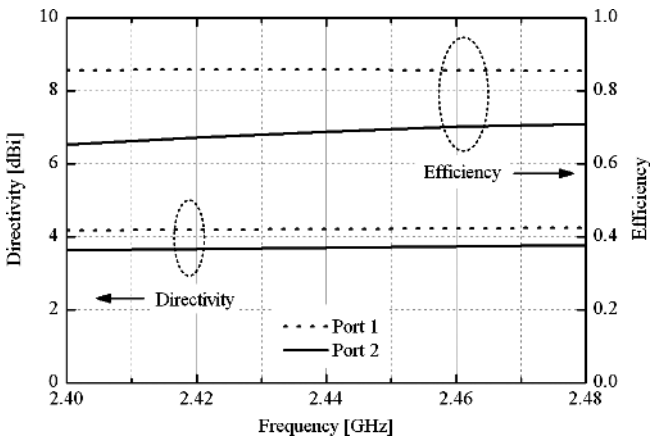

Fig. 23. Simulated directivity and efficiency of the proposed antenna.

horizontal polarization. Low cross-polarization level is also achieved for both polarizations.

Fig. 22 shows the measured gain of the proposed antenna compared with the simulation results. In the band of 2.4–2.48 GHz, the gain of vertical polarization is greater than 3.17 and 1.19 dBi for horizontal polarization. An average gain difference of 1.8 dB exists between dual polarizations. The reason is that the efficiency of horizontal polarization is lower than that of vertical polarization. The simulated directivity and efficiency of both polarizations are shown in Fig. 23. In the band of 2.4–2.48 GHz, the efficiency of vertical polarization is higher than 85.5% and 65.3% for horizontal polarization. As discussed in Section II-A, the back cavity serves as a shunt capacitance and affects the impedance matching of vertical slot. Therefore, the radiation efficiency is lower than a regular slot.

C. Diversity Performance

The correlation coefficient, the mean effective gain ratio, and the achievable diversity gain are the most important measures of multiple antennas in MIMO systems [21]–[26]. In this part, the complex correlation coefficient, and the mean effective gain (MEG) ratio are briefly evaluated based on the simulated results. The diversity performance of the proposed antenna is calculated in terms of diversity gains using Maximum Radio Combiner (MRC) by interacting with a statistical propagation model.

TABLE III
CORRELATION COEFFICIENT AND MEG RATIO

XPR	Γ = 6 dB	Γ = 0 dB	Γ = -6 dB
ρ_c	0.013	0.0021	0.0417
MEG_1 (vertical polarization)	-1.71 dB	-3.69 dB	-7.43 dB
MEG_2 (horizontal polarization)	-8.80 dB	-4.85 dB	-2.81 dB
$\lvert MEG_1/MEG_2 \rvert$	7.09 dB	1.16 dB	4.62 dB

The proposed antenna is potentially applicable in indoor MIMO systems, where the reflection and diffraction are rich and the channel response is Rayleigh-distributed. In this environment, the multipatch signal is assumed 3-D uniform distributed in a full sphere. The complex correlation coefficient and envelope correlation coefficient in this environment is computed as [21], [22]

$$\rho_e \approx |\rho_c|^2 = \left| \frac{\oiint A_{12}(\Omega)\,\mathrm{d}\Omega}{\sqrt{\oiint A_{11}(\Omega)\mathrm{d}\Omega \oiint A_{22}(\Omega)\mathrm{d}\Omega}} \right|^2 \quad (1)$$

where

$$A_{ij} = \Gamma E_{\theta,i}(\Omega) E^*_{\theta,j}(\Omega) \cdot p_\theta(\Omega) + E_{\phi,i}(\Omega) E^*_{\phi,j}(\Omega) p_\phi(\Omega) \quad (2)$$

in which $E\theta$ and $E\phi$ denote the θ and ϕ components of the complex electrical field, Γ is the average cross-polarization ratio (XPR), the power ratio of vertical polarization and horizontal polarization, and $p_\theta(\Omega)$ and $p_\phi(\Omega)$ are the multipath angular density function of the θ and ϕ polarization.

The MEG ratio is derived as [23]–[25]

$$\mathrm{MEG}_i = \oiint \left[\frac{\Gamma}{1+\Gamma} G_{\theta,i}(\Omega)\, p_\theta(\Omega) + \frac{1}{1+\Gamma} G_{\phi,i}(\Omega)\, p_\phi(\Omega) \right] \mathrm{d}\Omega \quad (3)$$

in which $G_{\theta,i}(\Omega)$ and $G_{\phi,i}(\Omega)$ are the spherical power gain of the ith element of the θ and ϕ polarization. The calculated complex correlation coefficient and the MEG ratio of the proposed antenna in a uniform propagated environment are listed in Table III. For $\Gamma = 6$ dB, the incident wave is mainly vertical polarized. Most of the energy is received by the horizontal slot with the vertical polarization. MEG_1 is much bigger than MEG_2. For $\Gamma = 0$ dB, the powers of the vertical and horizontal polarized incident wave are statically equal. The difference between MEG_1 and MEG_2 is mainly contributed from the radiation efficiency. Seen from the results, the proposed dual-polarized antenna shows good performance in the indoor environment, where $\Gamma \cong 0$ dB.

The receive signals by different slot antennas are combined by using MRC, and the combined gains are compared to the ones received by each single slot. In each simulation, 10 000 round random channels are generated to study the performance of diversity. In each channels, 100 multipaths are generated, which

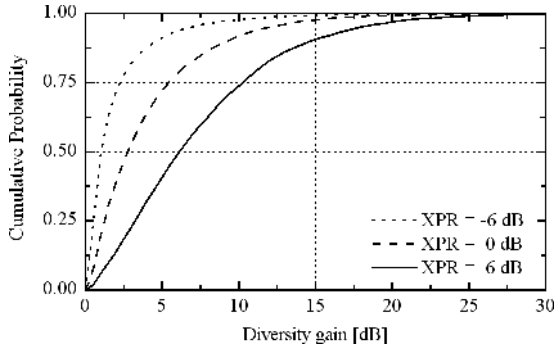

Fig. 24. CDF of the diversity gain using the proposed antenna compared to the single horizontal slot of the proposed antenna.

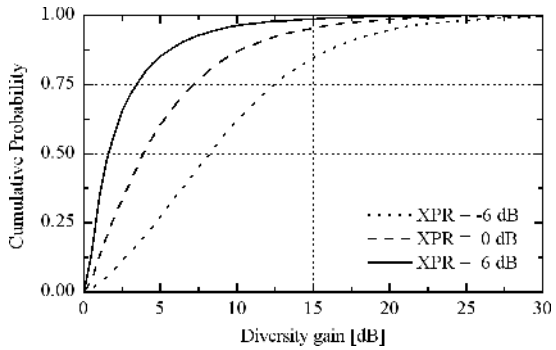

Fig. 25. CDF of the diversity gain using the proposed antenna compared to the single vertical the proposed antenna.

TABLE IV
OUTAGE DIVERSITY GAIN AT 1% PROBABLITY

Reference antenna	XPR		
	Γ = 6 dB	Γ = 0 dB	Γ = -6 dB
Horizontal slot (vertical polarization)	3.98 dB	5.74 dB	6.99 dB
Vertical slot (horizontal polarization)	7.46 dB	6.17 dB	4.77 dB

randomly distributed in the whole spherical angle and with identical and independent complex Gaussian distribution. The cumulative distribution functions (CDFs) of the diversity gain are shown in Figs. 24 and 25. The calculated diversity gain in this paper is the effective diversity gain, considering the radiation efficiency for both two polarizations [26].

The outage level at 1% probability of diversity gain is also calculated by comparing the outage level at 1% probability of the power received by the reference antenna and the proposed antenna. Single vertical polarization or horizontal polarization slot is used as the reference antenna. The calculated results are shown in Table IV. Good diversity gain is achieved when the vertical and horizontal components are almost equal. The outage level at 1% probability of diversity gain is greater than 5.74 dB in the indoor environment by using the proposed dual-polarized MIMO antenna.

IV. CONCLUSION

This paper proposed a dual-polarized MIMO antenna with omnidirectional radiation pattern in the azimuthal plane. Two orthogonally arranged colocated slots are designed to provide vertical and horizontal polarizations. The omnidirectional pattern is achieved by cutting the slots onto the walls of a slender columnar cuboid. In a small volume of $83 \times 11 \times 11$ mm^3 $(0.664\lambda_0 \times 0.088\lambda_0 \times 0.088\lambda_0)$, the isolation between dual operating modes is lower than -33.5 dB, whose 10-dB bandwidths of reflection coefficient cover the 2.4-GHz WLAN band. The gains of each polarization are greater than 3.17 and 1.19 dBi, respectively. The proposed dual-polarized antenna shows the merits of omnidirectional coverage, small volume, high port isolation, and low cross polarization. It shows the potential application in WLAN MIMO antenna design, especially in the volume-limited systems, such as portable access points and mobile terminals.

REFERENCES

[1] J.-M. Molina-Garcia-Pardo, J.-V. Rodriguez, and L. Juan-Llacer, "Polarized indoor MIMO channel measurements at 2.45 GHz," *IEEE Trans. Antennas Propag.*, vol. 56, no. 12, pp. 3818–3828, Dec. 2008.

[2] J. F. Valenzuela-Valdés, M. A. García-Fernández, A. M. Martí González, and D. A. Sánchez-Hernández, "Evaluation of true polarization diversity for MIMO systems," *IEEE Trans. Antennas Propag.*, vol. 57, no. 9, pp. 2746–2755, Sep. 2009.

[3] D. G. Landon and C. M. Furse, "Recovering handset diversity and MIMO capacity with polarization-agile antennas," *IEEE Trans. Antennas Propag*, vol. 55, no. 11, pp. 3333–3340, Nov. 2007.

[4] T. Brown, "Indoor MIMO measurements using polarization at the mobile," *IEEE Antennas Wireless Propag. Lett.*, vol. 7, pp. 400–403, 2008.

[5] A. S. Konanur, K. Gosalia, S. H. Krishnamurthy, B. Hughes, and G. Lazzi, "Increasing wireless channel capacity through MIMO systems employing co-located antennas," *IEEE Trans. Microw. Theory Tech.*, vol. 53, no. 6, pp. 1837–1844, Jun. 2005.

[6] H. Wong, K.-L. Lau, and K.-M. Luk, "Design of dual-polarized L-probe patch antenna arrays with high isolation," *IEEE Trans. Antennas Propag.*, vol. 52, no. 1, pp. 45–52, Jan. 2004.

[7] S.-C. Gao, L.-W Li, M.-S. Leong, and T.-S. Yeo, "Dual-polarized slot-coupled planar antenna with wide bandwidth," *IEEE Trans. Antennas Propag.*, vol. 51, no. 3, pp. 441–448, Mar. 2003.

[8] Y.-X. Guo, K.-W. Khoo, and L. C. Ong, "Wideband dual-polarized patch antenna with broadband baluns," *IEEE Trans. Antennas Propag.*, vol. 55, no. 1, pp. 78–83, Jan. 2007.

[9] Y. Li, Z. Zhang, W. Chen, Z. Feng, and M. F. Iskander, "A dual-polarization slot antenna using a compact CPW feeding structure," *IEEE Antennas Wireless Propag. Lett.*, vol. 9, pp. 191–194, 2010.

[10] E. A. Soliman, M. S. Ibrahim, and A. K. Abdelmageed, "Dual-polarized omnidirectional planar slot antenna for WLAN applications," *IEEE Trans. Antennas Propag.*, vol. 53, no. 9, pp. 3093–3097, Sep. 2005.

[11] T. J. Judasz and B. B. Balsley, "Improved theoretical and experimental models for the coaxial colinear antenna," *IEEE Trans. Antennas Propag.*, vol. 37, no. 3, pp. 289–296, Mar. 1989.

[12] R. Bancroft and B. Bateman, "An omnidirectional planar microstrip antenna," *IEEE Trans. Antennas Propag.*, vol. 52, no. 11, pp. 3151–3153, Nov. 2004.

[13] F.-R. Hsiao and K.-L. Wong, "Omnidirectional planar folded dipole antenna," *IEEE Trans. Antennas Propag*, vol. 52, no. 7, pp. 1898–1902, Jul. 2004.

[14] K.-L. Wong, F.-R. Hsiao, and T.-W. Chiou, "Omnidirectional planar dipole array antenna," *IEEE Trans. Antennas Propag.*, vol. 52, no. 2, pp. 624–628, Feb. 2004.

[15] W. Hong and K. Sarabandi, "Low profile miniaturized planar antenna with omnidirectional vertically polarized radiation," *IEEE Trans. Antennas Propag.*, vol. 56, no. 6, pp. 1533–1540, Jun. 2008.

[16] C. A. Balanis, *Antenna Theory: Analysis and Design*, 3rd ed. Hoboken, NJ: Wiley-Interscience, 2005.

[17] C.-C. Lin, L.-C. Kuo, and H.-R. Chuang, "A horizontally polarized omnidirectional printed antenna for WLAN applications," *IEEE Trans. Antennas Propag.*, vol. 54, no. 11, pp. 3551–3556, Nov. 2006.

[18] C.-H. Ahn, S.-W. Oh, and K. Chang, "A dual-frequency omnidirectional antenna for polarization diversity of MIMO and wireless communication applications," *IEEE Antennas Wireless Propag. Lett.*, vol. 8, pp. 966–969, 2009.

[19] A. L. Borja, P. S. Hall, Q. Liu, and H. Iizuka, "Omnidirectional loop antenna with left-handed loading," *IEEE Antennas Wireless Propag. Lett.*, vol. 6, pp. 495–498, 2007.
[20] A. Ando, A. Kondo, and S. Kubota, "A study of radio zone length of dual-polarized omnidirectional antennas mounted on rooftop for personal handy-phone system," *IEEE Trans. Veh. Technol.*, vol. 57, no. 1, pp. 2–10, Jan. 2008.
[21] R. Clarke, "A statistical theory of mobile radio reception," *Bell Syst. Tech. J.*, no. 2, pp. 957–1000, 1996.
[22] S. C. K. Ko and R. D. Murch, "Compact integrated diversity antenna for wireless communications," *IEEE Trans. Antennas Propag.*, vol. 49, no. 6, pp. 954–960, Jun. 2001.
[23] T. Taga, "Analysis for mean effective gain of mobile antennas in land mobile radio environments," *IEEE Trans. Veh. Technol.*, vol. 39, no. 2, pp. 117–131, May 1990.
[24] R. Vaughan and J. Andersen, "Antenna diversity in mobile communications," *IEEE Trans. Veh. Technol.*, vol. 36, no. 4, pp. 149–172, Nov. 1987.
[25] Y. Gao, X. chen, Z. Ying, and C. Parini, "Design and performance investigation of a dual-element pifa array at 2.5 GHz for MIMO terminal," *IEEE Trans. Antennas Propag.*, vol. 55, no. 12, pp. 3422–3440, Dec. 2007.
[26] P.-S. Kildal, K. Rosengren, J. Byun, and J. Lee, "Definition of effective diversity gain and how to measure it in a reverberation chamber," *Microw. Opt. Technol. Lett.*, vol. 34, no. 1, pp. 56–59, Jul. 2002.

Yue Li (S'11) was born in Shenyang, China, in 1984. He received the B.S. degree in telecommunication engineering from the Zhejiang University, Zhejiang, China, in 2007, and is currently pursuing the Ph.D. degree in electrical engineering from Tsinghua University, Beijing, China.

His current research interests include antenna design and theory, particularly in reconfigurable antennas, electrically small antennas, and antenna in package.

Zhijun Zhang (M'00–SM'04) received the B.S. and M.S. degrees from the University of Electronic Science and Technology of China, Chengdu, China, in 1992 and 1995, respectively, and the Ph.D. degree from Tsinghua University, Beijing, China, in 1999, all in electrical engineering.

In 1999, he was a Postdoctoral Fellow with the Department of Electrical Engineering, University of Utah, Salt Lake City, where he was appointed a Research Assistant Professor in 2001. In May 2002, he was an Assistant Researcher with the University of Hawaii at Manoa, Honolulu. In November 2002, he joined Amphenol T&M Antennas, Vernon Hills, IL, as a Senior Staff Antenna Development Engineer and was then promoted to the position of Antenna Engineer Manager. In 2004, he joined Nokia, Inc., San Diego, CA, as a Senior Antenna Design Engineer. In 2006, he joined Apple, Inc., Cupertino, CA, as a Senior Antenna Design Engineer and was then promoted to the position of Principal Antenna Engineer. Since August 2007, he has been with Tsinghua University, where he is a Professor with the Department of Electronic Engineering. He is the author of *Antenna Design for Mobile Devices* (Wiley, 2011).

Prof. Zhang is serving as Associate Editor of the IEEE TRANSACTIONS ON ANTENNAS AND PROPAGATION and IEEE ANTENNAS AND WIRELESS PROPAGATION LETTERS.

Jianfeng Zheng received the B.S. and Ph.D. degrees from Tsinghua University, Beijing, China, in 2002 and 2009.

He is currently an Assistant Researcher with the State Key Laboratory on Microwave and Digital Communications, Tsinghua University. His current research interests include spatial temporal signal processing, MIMO channel measurements, and antenna arrays for MIMO communications.

Zhenghe Feng (M'05–SM'08–F'12) received the B.S. degree in radio and electronics from Tsinghua University, Beijing, China, in 1970.

Since 1970, he has been with Tsinghua University as an Assistant, Lecturer, Associate Professor, and Full Professor. His main research areas include numerical techniques and computational electromagnetic, RF and microwave circuits and antenna, wireless communications, smart antenna, and spatial temporal signal processing.